

Noble gases in oxidized residue prepared from the Saratov L4 chondrite and Raman spectroscopic study of residues to characterize phase Q

Jun-ichi MATSUDA^{1*}, Kazuhiko MORISHITA¹, Masayuki NARA², and Sachiko AMARI³

¹Department of Earth and Space Science, Graduate School of Science, Osaka University, Toyonaka, Osaka 560-0043, Japan

²Laboratory of Chemistry, College of Liberal Arts and Sciences, Tokyo Medical and Dental University, Chiba 272-0827, Japan

³McDonnell Center for the Space Sciences and the Physics Department, Washington University, St. Louis, Missouri 63130, USA

*Corresponding author. E-mail: matsuda@ess.sci.osaka-u.ac.jp

(Received 11 October 2014; revision accepted 10 October 2015)

Abstract—We analyzed noble gases in an oxidized residue prepared from a HF-HCl residue of the Saratov L4 chondrite. The Ar, Kr, and Xe concentrations in the oxidized residue are two orders of magnitude lower than those in the HF-HCl residue, and they are close to concentrations in the bulk. The He and Ne concentrations are similar in the three samples. The Ne isotopic ratios are almost purely cosmogenic, indicating absence of presolar diamonds (the carrier of the HL component). Thus, Saratov contains phase Q without presolar diamond. A study of the Raman spectroscopic parameters for the HF-HCl residue and the oxidized residue shows large changes due to oxidation. The directions of these changes are the same as observed in Allende, except oxidation increased the I_D/I_G (intensity ratio of the D band to the G band) in Saratov but decreased in Allende. This difference may be attributed to the different crystalline stages of carbon in both meteorites. The shifts in the Raman parameters to a discrete and/or more expanded region suggest that (1) oxidation changes the crystalline condition of graphitic carbon, (2) phase Q is not a dissolved site, and (3) the release of Q-gas is simply related to the rearrangement of the carbon structure during oxidation.

INTRODUCTION

Study of noble gases is one of the important fields of earth and planetary sciences. The study of trapped components of noble gases plays an important role in the detection of presolar grains in meteorites. There are several trapped components of noble gases with distinct isotopic compositions. One of the most important is “Q,” which is named for “quintessence” because the phase was not clearly identified when it was found (Lewis et al. 1975). Using a chemical separation method, Lewis et al. (1975) showed that a small portion (0.02–0.04 wt%) of bulk Allende contains almost all of the heavy noble gases. The noble gases in this fraction are isotopically “normal” but are elementally fractionated, as they are more highly enriched in heavier noble gases compared to those of solar composition. This minor phase is called “Q” or type “P1” (Huss and Lewis 1994).

Subsequent work showed that phase Q is present in carbonaceous chondrites (Alaerts et al. 1979a; Matsuda et al. 1980), ordinary chondrites (Alaerts et al. 1979b; Moniot 1980), and even in the graphite nodule in the Canyon Diablo iron meteorite (Matsuda et al. 2005). Thus, it is likely that Q-gas was ubiquitously present in the early solar system. The chemical structure of phase Q is not clearly understood, although it is carbonaceous (Reynolds et al. 1978; Ott et al. 1981). As phase Q is the main carrier of primordial heavy noble gases in the solar system, its clear identification is important for studying early solar system processes.

Furthermore, phase Q should be a very minor carbon phase in mass that is different from the major carbon, as indicated by the differences in the release pattern of major carbon versus noble gases in the ordinary chondrite Dhajala (Schelhaas et al. 1990) and in enstatite chondrites (Verchovsky et al. 2002), although the temperature interval over which most of

the gases are released coincides with the combustion of most of the carbon in Allende (Frick and Pepin 1981).

Marrocchi et al. (2005) reported that the low temperature fractions of Q-gases in the Orgueil residue were lost through pyridine treatment. In contrast Busemann et al. (2008) and Spring et al. (2010) did not observe a significant difference in noble gas concentrations between pyridine-treated and untreated residues in other primitive chondrites. Matsuda et al. (2010a) indicated that loss of Q-gases was only the case for Orgueil and that it was due to the loss of some kind of organic matter that formed and adsorbed the fractionated Q- and HL gases during aqueous alteration of Orgueil's parent body. However, Spring et al. (2011) did not observe a significant loss of Q-gases even in Orgueil.

Phase Q is resistant to HF-HCl but not to oxidation, and it has not yet been isolated as an independent phase. For this reason, the Q-gas component has mostly been derived from the difference between the noble gas components in the HF-HCl residue and its oxidized residue. The latter is obtained using an oxidant such as HNO₃, Na₂Cr₂O₇, or H₂O₂. Wieler et al. (1991, 1992) directly determined the Q-gas component using a closed-system etching experiment and analyzing the noble gases derived during oxidation. Matsuda et al. (1999) found that a floating fraction during the freeze-thaw disaggregation is similar to the HF-HCl residue in noble gas concentrations and in isotopic compositions, except for the ¹²⁹Xe/¹³²Xe ratio, which was much higher in the floating fraction. The high ¹²⁹Xe/¹³²Xe ratio in the HF-HCl residue is supposedly due to the readsorption of ¹²⁹Xe from iodine minerals during chemical separation, which did not occur during physical separation. Matsuda et al. (1999) succeeded in obtaining material similar to the chemical residue using the physical method but did not obtain phase Q in its isolated state. The mechanism of floating such a fraction is still unclear, but the authors supposed that phase Q is always associated with presolar diamonds except for the oxidation. They also considered that presolar diamonds float up during ultrasonic vibration because the adhesion of water to diamonds is very weak.

The primordial noble gases in phase Q and other carriers of noble gases decrease with increasing petrologic subtype among type 3 ordinary chondrites, indicating that the thermal metamorphism in parent bodies affects these phases to varying degrees (Huss et al. 1996). Thermal metamorphism most readily attacks SiC (carrier of Ne-E(H), Kr-S, and Xe-S) and then presolar diamonds (carrier of HL gases). Phase Q is more resistant compared to the other two carriers (Huss et al. 1996) and it alone is present although

presolar diamonds and SiC are absent in ordinary chondrites of petrologic type >3.8 (Alexander et al. 1990; Huss 1990).

Phase Q is difficult to separate from presolar diamonds in laboratory experiments without being dissolved. These two materials can be well separated in the solar system, as shown in the Saratov (L4) meteorite and explained below and further investigated in this work. Matsuda et al. (2010b) measured noble gases of the bulk and HF-HCl residue of the Saratov (L4) chondrite using stepwise heating and confirmed the presence of phase Q and the absence of presolar diamonds in type 4 ordinary chondrites (Alexander et al. 1990; Huss 1990). Interestingly, the Ne isotopic ratios lay on a straight line connecting the cosmogenic component and a component in composition between Ne-Q (Wieler et al. 1992) and Ne-HL (Huss and Lewis 1994). This led to the idea that Ne-Q in Saratov may have been changed by incorporating Ne-HL during the thermal metamorphism. However, differences in Ne-Q are also observed in other chondrites and there is no correlation between the ²⁰Ne/²²Ne ratios of Ne-Q and the petrologic types (Busemann et al. 2000). Thus, we concluded that the Ne-Q in Saratov is intrinsically different from that in other chondrites. Amari et al. (2013) further performed a colloidal separation of the HF-HCl residue of Saratov, and obtained the highest ¹³²Xe concentration ever observed in one of the fractions after several steps. They concluded that phase Q is associated with only a minor component of the porous carbon.

In this study, we measured the concentrations of all noble gases and the isotopic compositions of light noble gases in the oxidized HF-HCl-resistant residue of the Saratov (L4) chondrite. Of interest was the examination of the type of noble gas signatures obtained after phase Q is dissolved in a residue that contains only phase Q as a primordial component of noble gases. We then performed Raman spectroscopy for the HF-HCl residue and its oxidized residue. The results are compared with those from a similar study on Allende residues (Matsuda et al. 2010c) in order to better characterize and understand phase Q.

SAMPLE PREPARATION

The chemical leaching was conducted at Washington University in St. Louis using the procedure in Fig. 1. We first prepared an original HF-HCl-resistant residue (AB) by dissolving L4 Saratov bulk (7.1655 g) with seven alternating cycles of 10M HF-1M HCl and 6M HCl (one day each). Then, we used CS₂ to remove elemental sulfur. The yield of the residue (AC) was 0.76 wt% (estimated error of 20%). The residue

Chemical treatment of Saratov A (7.1655 g)

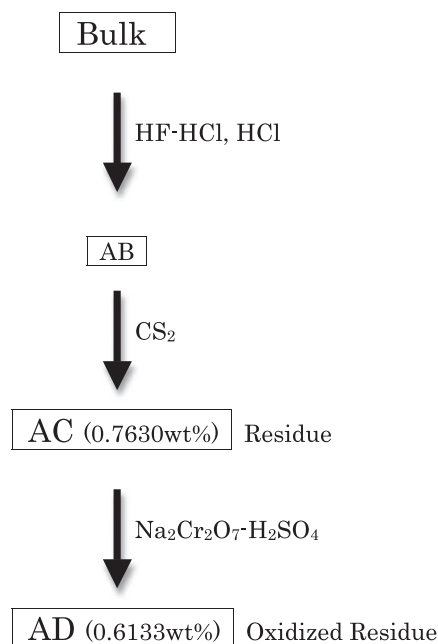


Fig. 1. Schematic diagram of sample preparation for the oxidized residue AD and the residue AC of the Saratov L4 chondrite. The abundance is relative to the bulk sample.

AC was further treated with 0.083M $\text{Na}_2\text{Cr}_2\text{O}_7$ -1M H_2SO_4 at 77 °C for 10 h to destroy Q, yielding the oxidant residue AD. The AD yield relative to the bulk Saratov was 0.61 wt%. Thus, it appears that about 20 wt% of AC was dissolved by oxidation. However, this number has a large uncertainty considering that the yields of the individual fractions of AD and AC have uncertainties in the range of 20%.

EXPERIMENTAL PROCEDURES

The noble gas measurements were performed at Osaka University. Results for the bulk sample and the AC separate have been previously reported in Matsuda et al. (2010b) along with a detailed description of the experimental procedures. Samples were heated in a Mo crucible with a Ta heater for 20 min at each temperature step. The noble gases were measured using a sector-type mass spectrometer VG5400. The concentrations and isotopic ratios of the noble gases in the bulk sample and the AC separate were measured by stepwise heating at 600, 800, 1000, 1200, 1400, and 1600 °C (Matsuda et al. 2010b). In this study, we measured the concentrations in the oxidized residue AD of all noble gases and the isotopic ratios for the light noble gases (He, Ne, and Ar) in fewer release steps, at

600, 1000, 1200, and 1600 °C only. This was because of the small quantities of gas analyzed due to the small mass of the sample and the small gas concentrations in AD. Hot blanks were measured at 1000 and 1600 °C, and for correction we applied the 1000 °C blank for the 600 and 1000 °C extractions, and the 1600 °C blank for the 1200 and 1600 °C extractions. Procedural hot blanks at 1600 °C were: $^4\text{He} = 8.5 \times 10^{-10}$, $^{22}\text{Ne} = 6.2 \times 10^{-13}$, $^{36}\text{Ar} = 1.1 \times 10^{-11}$, $^{84}\text{Kr} = 1.1 \times 10^{-12}$, and $^{132}\text{Xe} = 9.9 \times 10^{-14} \text{ cm}^3\text{STP}$.

The Raman spectroscopic study was performed at Tokyo Medical and Dental University. Precise descriptions of the experiments and band fitting are given in Matsuda et al. (2009, 2010c) and Nagashima et al. (2012). In this study, the Raman spectrum was obtained from 10 accumulations of 30 s each using an excitation wavelength of 532 nm (Nd:YAG laser, laser power of 1.5–2.4 mW, Kaiser Optical Systems, Inc.). The excitation laser spot size was approximately 2 μm in diameter. A high laser power changes the sample to a more amorphous state for the carbon material of a carbonaceous chondrite like Allende (Matsuda et al. 2009; Morishita et al. 2011); however, 1.5–2.4 mW does not have a large effect on the carbon in ordinary chondrites. Even for the carbon material in carbonaceous chondrite Allende, the positions of the D and G bands shift downward by only 3–4 cm^{-1} at this laser power (Morishita et al. 2011). For both natural and artificial graphite, the laser-induced downward shift of the G band is much less than for Allende (Kagi et al. 1994). We suppose that this effect is smaller in the carbon material in ordinary chondrites because its graphitization is higher than in carbonaceous chondrites (Busemann et al. 2007).

RESULTS AND DISCUSSION

Noble Gases

The results for noble gases in AD (oxidized residue) are shown in Table 1, where they are compared with the data of the bulk sample and the AC residue obtained earlier by Matsuda et al. (2010b). The errors in the concentrations of noble gases are about 10%, including the error of the line volume. The uncertainty in the blank concentrations was taken to be 100%. In cases where the blank corrections were higher than 50%, we show the concentration with upper limits. All Kr data are given as upper limits.

Figure 2 shows the elemental concentrations in the bulk, AC, and AD. The Ar, Kr, and Xe concentrations in AD are two orders of magnitude lower than those in AC and are close to those in the bulk, whereas the He and Ne concentrations are similar in all three samples

Table 1. Concentrations and isotopic ratios of He, Ne, Ar, Kr, and Xe in the Saratov oxidized residue.

Sample	Temp. [°C]	[⁴ He] 10 ⁻⁶ cm ³ STP g ⁻¹	³ He/ ⁴ He ×10 ⁻⁴	[²² Ne] 10 ⁻⁸ cm ³ STP g ⁻¹	²⁰ Ne/ ²² Ne	²¹ Ne/ ²² Ne	[³⁶ Ar] 10 ⁻⁸ cm ³ STP g ⁻¹	³⁸ Ar/ ³⁶ Ar	⁴⁰ Ar/ ³⁶ Ar	[⁸⁴ Kr] 10 ⁻¹⁰ cm ³ STP g ⁻¹	[¹³² Xe] 10 ⁻¹⁰ cm ³ STP g ⁻¹	Reference
AD (4.0 mg)	600	17	158.5 ± 5.5	1.3	1.018 ± 0.065	0.860 ± 0.017	1.2	0.2152 ± 0.0026	69.8 ± 2.2	<2.2	3.1	
Oxidized residue	1000	1.7	135.5 ± 34.2	3.6	0.895 ± 0.036	0.834 ± 0.014	1.1	0.3464 ± 0.0038	21.0 ± 0.8	<2.2	2.3	
	1200	0.39	109.3 ± 56.5	0.83	1.054 ± 0.123	0.843 ± 0.024	1.1	0.4348 ± 0.0052	<27	<3.2	3.1	
	1600	0.25	–	0.38	1.324 ± 0.284	0.901 ± 0.042	1.3	0.3778 ± 0.0044	16 ± 1	<2.6	3.5	
Total	20	20	153.5 ^a ± 5.8	6.2	0.969 ± 0.035	0.845 ± 0.010	4.6	0.3427 ± 0.0020	<33.4	<10	12	
AC (3.63 mg)	Total	26	113.5 ± 2.2	6.1	2.739 ± 0.034	0.678 ± 0.004	335	0.1934 ± 0.0002	9.9 ^b ± 0.1	521	1060	Matsuda et al. (2010b)
Residue												
Bulk (248.7 mg)	Total	22	206.5 ± 4.9	10	0.799 ± 0.004	0.859 ± 0.003	6.8	0.2835 ± 0.0004	889.0 ± 9.3	6.9	17	Matsuda et al. (2010b)
Q			1.23–1.59		10.05–10.70	0.0291–0.0321		0.18727				Busemann et al. (2000)
HL ^c			1.70		8.5	0.036		0.2270	<0.08			Huss and Lewis (1994)
Cosmogenic ^d			2000		0.85	0.92		1.47				Ozima and Podosek (1983)
Air			0.01399		9.80	0.029		0.188	295.5			Schultz et al. (1991)

The elemental concentrations are listed as upper limits without blank correction in the case that the blank exceed 50%.

^aThe total is the sum without 1600 °C fraction.

^bThe total is the sum of 600, 800, and 1000 °C fractions.

^cThis HL component of Ne (Ne-HL) is actually Ne-A2 (Ne-HL + P6) (Huss et al. 1996).

^dThese are representative values. Schultz et al. (1991) is for Ar.

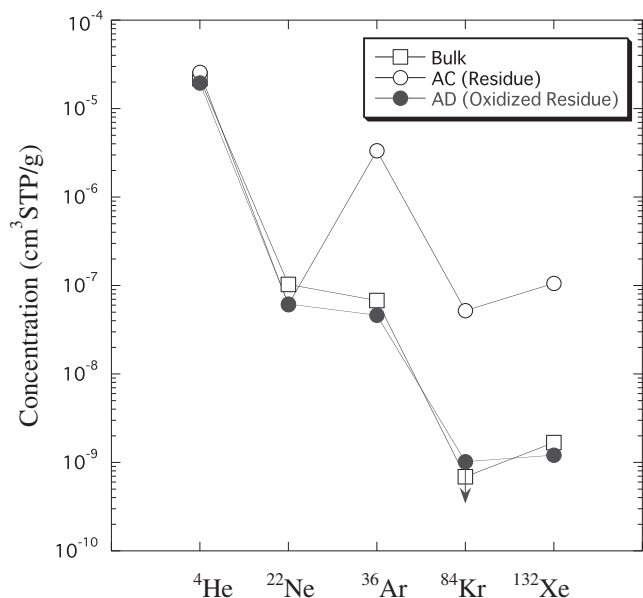


Fig. 2. Comparison of the total elemental concentrations of noble gases in the bulk (open squares), the residue AC (open circles), and the oxidized residue AD (closed circles) of L4 Saratov. The data for the bulk and AC are from Matsuda et al. (2010b).

(Fig. 2). This suggests that the heavy noble gases are mainly in AC and that the gases were lost in AD by oxidation, indicating that phase Q was removed by oxidation. The whole pattern of noble gases is similar in AD and in the bulk, but the concentrations are slightly lower in AD. The sample weight for the measurement of the bulk was 248.7 mg (Matsuda et al. 2010b), and that of AD in this study is only 4 mg. Thus, this study analyzed about 1/62 of the amount of noble gases compared to the prior study of the bulk.

Figure 3 shows the release curves of individual noble gases in the bulk, AC, and AD fractions. We do not show ⁸⁴Kr because we have only upper limits. To compare these data to data in AD with temperature steps of 600, 1000, 1200, and 1600 °C, the 800 °C fraction was added to the 1000 °C fraction and the 1400 °C fraction was added to the 1600 °C fraction for the bulk sample and the AC fraction. The release patterns of ⁴He have maximum release at the lowest temperature (600 °C) step (Fig. 3a) and those of ²²Ne have 1000 °C peaks (Fig. 3b) for all samples. In contrast, ³⁶Ar (Fig. 3c) and ¹³²Xe (Fig. 3d) is released in AD in similar amounts for all temperature fractions. The release peak at 1200 °C that is observed in AC and that is supposedly from phase Q is not seen in the release pattern of fraction AD, indicating again that phase Q was present in AC but is not present in AD.

Figure 4 shows an Ne three-isotope plot. Considering that the cosmogenic component has a

range depending on target materials, one can see that Ne in AD is almost purely cosmogenic. The trapped component has been completely removed by oxidation. About 80%¹ of the total amount of ²²Ne is cosmogenic in AC (Matsuda et al. 2010b), but almost 100% is cosmogenic in AD. Thus, there is no phase Q nor Ne-HL in AD. Similar results of almost pure cosmogenic Ne are also reported for oxidized residues in other equilibrated ordinary chondrites with high petrologic types (Alaerts et al. 1979b; Moniot 1980). The cosmogenic component is also seen in the He and Ar isotopic ratios. Table 1 shows ³He/⁴He ratios that are in the range 10⁻² for all temperature steps although in addition radiogenic ⁴He is present, lowering this ratio. ³⁸Ar/³⁶Ar ratios of 0.2–0.4 indicate the presence of a cosmogenic component also for Ar (Table 1). The presence of a radiogenic component is shown by the ⁴⁰Ar/³⁶Ar ratios. We calculated the cosmogenic ³⁶Ar amounts assuming that it is a mixture of trapped (³⁶Ar/³⁸Ar)_{atm} = 5.32) and cosmogenic (³⁶Ar/³⁸Ar)_c = 0.68) components (Schultz et al. 1991). The cosmogenic ³⁶Ar is only 0.4% of the total ³⁶Ar in the residue (AC) and 7% in the bulk (Matsuda et al. 2010b), and this proportion increases to 12% in AD. The trapped component is still dominant for Ar for all samples, but the cosmogenic component is enriched in AD. As the ⁴⁰Ar/³⁶Ar ratio of the total Ar in AD is higher than that in AC (Table 1), the radiogenic components are enriched relative to the trapped component by oxidation. However, the absolute amount of radiogenic ⁴⁰Ar in the residue AC is much lower than that in the oxidized residue AD, indicating that radiogenic ⁴⁰Ar was largely dissolved during oxidation.

Although this estimate has very large errors due to the large errors in the individual mass yields of fractions AC and AD (each about 20%), we calculated the nominal concentrations of noble gases in phase Q based on the difference between AC and AD (Table 2). We also list for comparison in Table 2 the concentrations of noble gases in the fraction AJ. AJ is the fraction prepared from AC by Amari et al. (2013) using colloidal separation and it has the highest ¹³²Xe concentrations of 2.1 × 10⁻⁶ cm³ STPg⁻¹ among the Q-rich fractions that ever have been analyzed. Interestingly, the nominal concentrations of noble gases in phase Q from the calculation are lower than those in AJ. The differences are rather constant with a factor of 3–4 for ³⁶Ar, ⁸⁴Kr, and ¹³²Xe. For ⁴He and ²²Ne, concentrations in AC and AD are almost identical within error, and no reliable difference calculation can be performed. The weight fraction of AJ in bulk Saratov is 0.0288 wt% (Amari et al. 2013) and that of

¹This is written as 20% in Matsuda et al. (2010b), but it is a mistake.

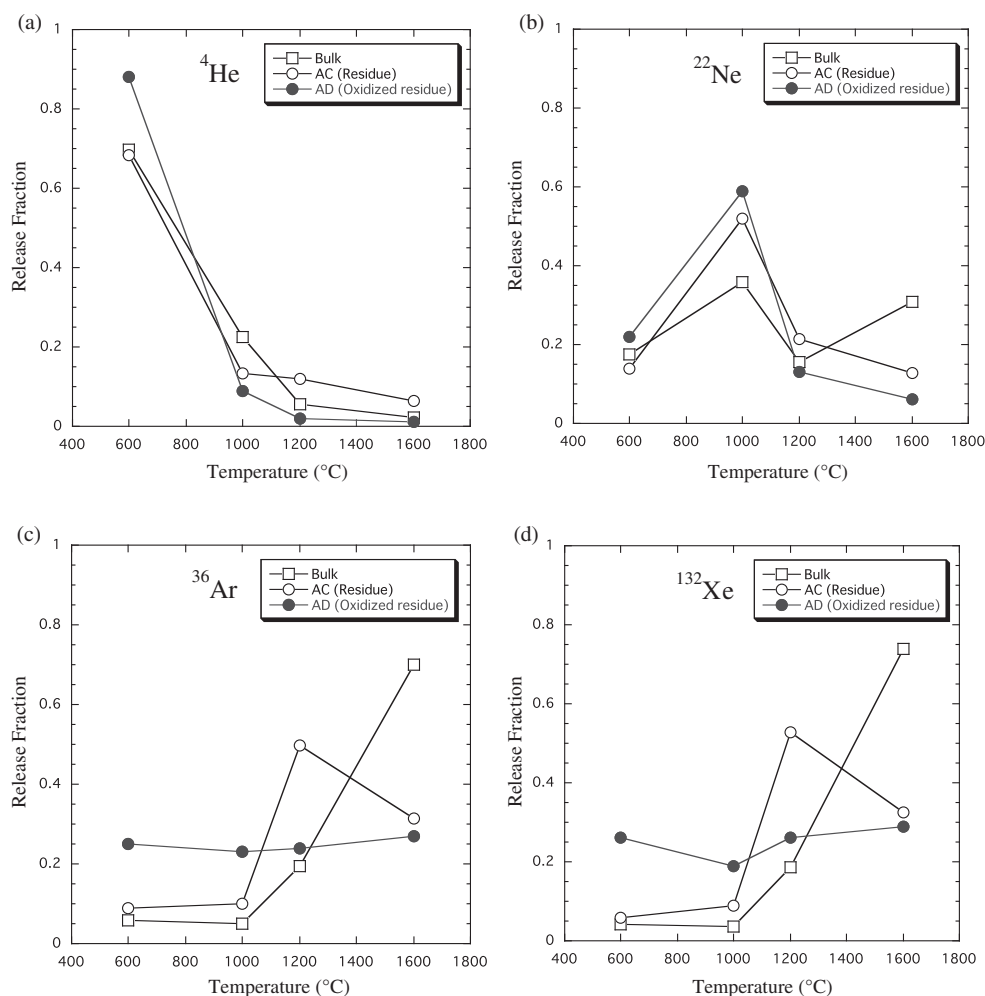


Fig. 3. Release profiles of (a) ^4He , (b) ^{22}Ne , (c) ^{36}Ar , and (d) ^{132}Xe in the bulk, AC, and AD of Saratov. Release fractions are normalized to the total gas amounts in individual samples. The data for the bulk and AC are from Matsuda et al. (2010b), where the temperature steps are 600, 800, 1000, 1200, 1400, and 1600 °C. To compare these data to data in AD with temperature steps of 600, 1000, 1200, and 1600 °C, the 800 °C fraction was added to the 1000 °C fraction and the 1400 °C fraction was added to the 1600 °C fraction.

the calculated phase Q is 0.1497 wt% (the difference between 0.7630 wt% of AC and 0.6133 wt% of AD) (Fig. 1). This difference is a factor of about five, and is close to the difference in the noble gas concentrations. Neglecting the significant uncertainty introduced from the weight uncertainties, this would suggest that the calculated phase Q is not a real phase Q but is diluted with another phase that has no noble gases, indicating that the oxidation dissolved some other carbon materials. A 20 wt% loss of AC during oxidation seems to be large compared to the 4–8 wt% loss for the type 3 carbonaceous chondrite Allende (Lewis et al. 1975). Bringing the data into context, Alaerts et al. (1979b) reported 2.2–13 wt% loss for LL chondrites, but Moniot (1980) reported 9–95 wt% for H chondrites. Thus, 20 wt% loss of Saratov (L4) during oxidation

seems possible. For the type 3 carbonaceous chondrites, the weight loss during oxidation is as high as 54 wt% for Grosnaja (Matsuda et al. 1980) and 42 wt% for Lancé (Alaerts et al. 1979a). It is noted that the concentration of cosmogenic ^{21}Ne in AD is about 20% higher than that in AC. This is equivalent to 20 wt% loss of carbonaceous material that has no cosmogenic ^{21}Ne during oxidation.

Raman Spectroscopy

Carbon material shows G and D bands in Raman spectroscopy. The G band is assigned to the fundamental E_{2g} vibration mode of the aromatic plane of graphite. Perfectly crystallized graphite only shows this band at 1580 cm^{-1} . The D band in graphite is

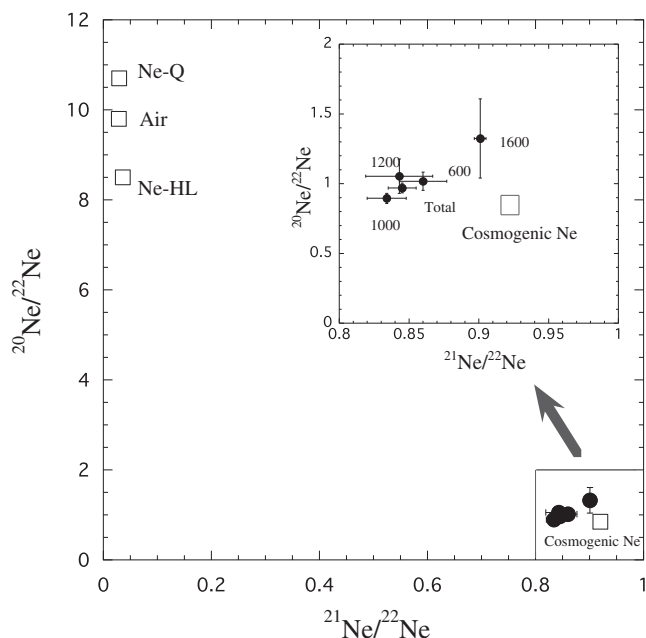


Fig. 4. Three-isotope plot showing $^{20}\text{Ne}/^{22}\text{Ne}$ versus $^{21}\text{Ne}/^{22}\text{Ne}$ for AD. The numerical values are the extraction temperatures ($^{\circ}\text{C}$) of the stepwise heating. The data source for Murchison Q is from Wieler et al. (1992), and that for HL is from Huss and Lewis (1994). The cosmogenic Ne is from Ozima and Podosek (1983).

related to structural defects (D indicates defect) and appears at about 1350 cm^{-1} . The D band is generally observed in nonperfectly crystallized carbon such as graphitic carbon, activated carbon, carbon black, etc. (Tuinstra and Koenig 1970).

Both G and D bands are observed for carbon material in meteorites. Furthermore, the band positions (ω_G and ω_D), peak intensities (I_G and I_D), and bandwidths (full width at half maximum; FWHM_G and FWHM_D) change depending on the crystalline degree of graphitic carbon. If the carbonaceous material is a composite of various kinds of graphitic carbon, the above parameters are composite of the individual parameters.

We plotted several parametric combinations in Fig. 5 to constrain the carbonaceous material in AC and AD. For comparison we also plotted Allende data (Matsuda et al. 2010c) with small symbols. The Raman parameters (especially, D band parameters) for Saratov show larger spreads than for Allende. Figure 5a compares the peak positions of the G and D bands. It is clear that both peak positions shift to higher values by oxidation. FWHM_G decreases and scatters widely (Fig. 5b), whereas FWHM_D increases slightly (Fig. 5c) after oxidation. Changes in the above four parameters observed in Saratov are very similar to those in Allende

(Matsuda et al. 2010c). In contrast, the I_D/I_G ratios increase after oxidation in Saratov (Fig. 5d) but in Allende they decrease. We compare the changes in Raman parameters for Allende and Saratov in Table 3.

It is interesting that the Raman parameters shift either to a discrete region (in Figs. 5a and 5c) or to a more expanded region (in Figs. 5b and 5d) after oxidation. The carbonaceous material in meteorites should be a composite of various types of disordered graphitic carbon, which have different crystalline degrees. If oxidation simply removes some types of carbon from AC, the shift in Raman parameters should be continuous and located in a region narrower than the region before oxidation. However, ω_D shifts to an upward region and ω_G increases and occupies a more expanded region (Fig. 5a). FWHM_D slightly increases (Fig. 5c), whereas FWHM_G decreases and both are spread out over a more extended region (Fig. 5b). The increases of both ω_D and FWHM_D indicate an increase in the disordering sites of graphitic carbon (Fig. 5c) where graphitic carbon is partly oxidized and/or the crystalline defect is increased after oxidation. Meanwhile, the increase in ω_G and the decrease in FWHM_G indicate that highly disordered carbon is oxidized and lost (Matsuda et al. 2010c). Thus, it is apparent that a complex reaction of dissolution and damage occurred during oxidation. Oxidation does not simply remove soluble carbon materials but rather also changes the graphitic carbon structure, as has already been reported for Allende (Matsuda et al. 2010c).

This is very different from the pyridine treatment of Orgueil where there is no effect on ω_D and FWHM_D (although there is a small lower shift in ω_G and a small increase in FWHM_G due to the swelling of the macromolecular network by pyridine) (Matsuda et al. 2010a).

We conclude that aggressive acid oxidation changes the whole carbon structure to a more amorphous (disordered) state in chondrites.

So far, it has been generally assumed that oxidation simply attacks the soluble carbon and that phase Q is a part of these dissolved carbon materials. Thus, the assumption is that the noble gases contained in phase Q are released during oxidation simply by the dissolution of the phase itself. However, Raman spectroscopy may lead us to a different conclusion. We consider it more likely that phase Q is some amorphous part of the carbon that is resistant to the oxidants and that the release of Q-gas simply results from the structural disordering and rearrangement of the carbon phase, as was shown in the Allende study (Matsuda et al. 2010c). Of course, we still cannot rule out the possibility that phase Q is a very minor discrete phase and it is always covered by the major disordered graphitic carbon

Table 2. Comparisons of the concentrations of noble gases in phase Q from the calculation and in AJ in Saratov.

Sample	[⁴ He] 10 ⁻⁶ cm ³ STP g ⁻¹	[²² Ne] 10 ⁻⁸ cm ³ STP g ⁻¹	[³⁶ Ar] 10 ⁻⁸ cm ³ STP g ⁻¹	[⁸⁴ Kr] 10 ⁻¹⁰ cm ³ STP g ⁻¹	[¹³² Xe] 10 ⁻¹⁰ cm ³ STP g ⁻¹	Reference
Phase Q (From the calculation)	51	5.8	1700	2600	5300	This study
AJ	99	28	6800	7300	21000	Amari et al. (2013)

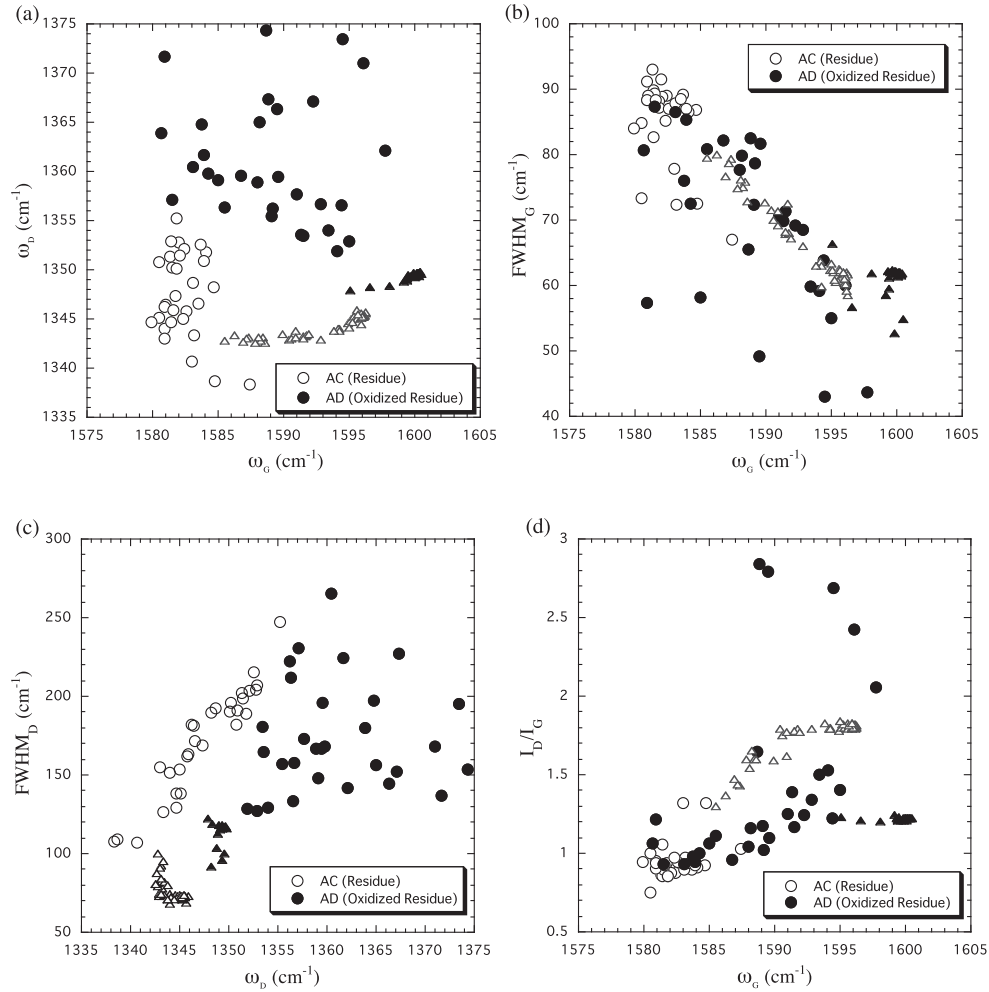


Fig. 5. Comparisons of Raman spectroscopic parameters for the residue AC (open circles) and the oxidized residue AD (closed circles). a) ω_D (peak position of D band) against ω_G (peak position of G band). b) FWHM_G (full width at half maximum of G band) against ω_G . c) FWHM_D (full width at half maximum of D band) against ω_D . d) I_D/I_G (peak intensity ratio of D and G bands) against ω_G for AC and AD. For comparison, we also show the data for Allende; the residue (open small triangles: AMD1 + AMD3 in Matsuda et al. 2010c) and the oxidized residue (closed small triangles: AMD2 in Matsuda et al. 2010c).

during the Raman spectroscopy observations (Matsuda et al. 2010c).

The changes in the Raman parameters by oxidation are very similar for Allende and Saratov except for the I_D/I_G ratios (Table 3). These ratios decrease after

oxidation in Allende (Matsuda et al. 2010c), but they increase in Saratov (Fig. 5d). This opposite behavior in the I_D/I_G ratios must be explained.

We suppose this phenomenon is related to the different crystalline stage of carbon material in these

Table 3. Comparisons of the changes in the Raman parameters by oxidation for Allende (Matsuda et al. 2010a) and Saratov (this study).

Raman parameters	Allende (CV3)	Saratov (L4)
ω_G	Upward shift	Upward shift
FWHM_G	Small downward shift	Downward shift
ω_D	Upward shift	Upward shift
FWHM_D	Upward shift	Small upward shift (no shift?)
I_D/I_G	Downward shift	Upward shift

two types of meteorites. Well-crystallized graphite has only a G band and no D band. As the amorphization proceeds, the D band appears and first increases but then decreases. Ferrari and Robertson (2000) described this change as corresponding to transformation from graphite to nanocrystalline graphite and from nanocrystalline graphite to amorphous carbon.

We suppose that the carbon materials in Saratov (L4) are in a more graphitized state than in Allende and are in the change of graphite to nanocrystalline graphite (Stage 1 in Ferrari and Robertson 2000). In this case, the amorphization (the direction from graphite to nanocrystalline graphite) causes an increase in the I_D/I_G ratios (Ferrari and Robertson 2000). In fact, the crystallite size of graphitic carbon has an inverse relation with the I_D/I_G ratio (Tuinstra and Koenig 1970). Thus, at this stage, the larger I_D/I_G ratios correspond to smaller crystallite size of graphitic carbon and amorphization leads to an increase in I_D/I_G ratios.

Allende is a carbonaceous chondrite of type CV3, and the crystalline state of carbon is in the stage of nanocrystalline graphite to amorphous carbon (Stage 2 in Ferrari and Robertson 2000). In Stage 2, carbon having a lower I_D/I_G ratios is in a more amorphous state. In fact, the I_D/I_G ratio decreased by the amorphization attributed to the effect of laser-induced heating at a higher laser power (Matsuda et al. 2009).

Thus, we conclude that the opposite change in the I_D/I_G ratios by oxidation is the result of the different crystalline stages of carbon in Allende and Saratov, and that oxidation changes the whole carbon structure into a more amorphous state in both cases.

SUMMARY

1. We prepared an oxidized residue (AD) of the Saratov L4 chondrite. The yield of AD is 0.61 wt% of bulk Saratov. The concentrations of heavy noble gases in AD are much lower than those in the Q-gas rich HF-HCl residue (AC) and are similar to (or slightly lower) than those in the bulk. The isotopic signature on Ne shows that Ne in AD is an

almost pure cosmogenic component. The presence of a cosmogenic component is also seen in He and Ar. Cosmogenic ^{36}Ar is 12% of total ^{36}Ar in AD, which is higher than in AC. Radiogenic components are present in He and Ar.

2. Nominal concentrations of noble gases in phase Q, calculated as the difference between those in AC and AD, are lower than those in AJ that was prepared from AC by colloidal separation. The obtained nominal depletion factor is similar to the difference in the mass fraction. Thus, we suppose that oxidation dissolved not only phase Q (in case phase Q is soluble), but also carbon material that has no noble gases.
3. From the discrete and expanded shifts in the Raman parameters, we conclude that oxidation not only dissolves some type of oxidizable carbon, but also changes the whole carbon structure into a more amorphous state.
4. The changes in the Raman parameters after oxidation in Saratov are the same as those in Allende, except that the I_D/I_G ratios increased in Saratov while it decreased in Allende. We suppose the different changes in the I_D/I_G ratios after oxidation are the result of the different crystalline stages of graphitic carbon in the two chondrites. It is reasonable to conclude that amorphization proceeds by oxidation in both cases.
5. It is very likely that the release of Q-gas is associated with the above structural change in meteoritic carbon during oxidation.

Acknowledgments—This study was supported by NASA grant NNX13A48G (S.A.). The paper benefitted greatly from reviews provided by Drs. A. Verchovsky, S. Crowther, U. Ott, and an anonymous reviewer. The authors also thank the handling editor Dr. I. Leya for his comments and editorial suggestions.

Editorial Handling—Dr. Ingo Leya

REFERENCES

- Alaerts L., Lewis R. S., and Anders E. 1979a. Isotopic anomalies of noble gases in meteorites and their origins—IV. C3 (Ornans) carbonaceous chondrites. *Geochimica et Cosmochimica Acta* 43:1421–1432.
- Alaerts L., Lewis R. S., and Anders E. 1979b. Isotopic anomalies of noble gases in meteorites and their origins—III. LL-chondrites. *Geochimica et Cosmochimica Acta* 43:1399–1415.
- Alexander C. M. O'D., Arden J. W., Ash R. D., and Pillinger C. T. 1990. Presolar components in the ordinary chondrites. *Earth and Planetary Science Letters* 99:220–229.
- Amari S., Matsuda J., Stroud R. M., and Chisholm M. F. 2013. Highly concentrated nebular noble gases in porous

- nanocarbon separates from the Saratov (L4) meteorite. *The Astrophysical Journal* 778: 37 (9 pp).
- Busemann H., Baur H., and Wieler R. 2000. Primordial noble gases in “phase Q” in carbonaceous and ordinary chondrites studied by closed-system stepped etching. *Meteoritics & Planetary Science* 35:949–973.
- Busemann H., Alexander C. M. O’D., and Nittler L. R. 2007. Characterization of insoluble organic matter in primitive meteorites by microRaman spectroscopy. *Meteoritics & Planetary Science* 42:1387–1416.
- Busemann H., Alexander C. M. O’D., Nittler L. R., and Wieler R. 2008. Noble gases in insoluble organic matter in the very primitive meteorites Bells, EET 92042 and GRO 95577 (abstract #1777). 39th Lunar and Planetary Science Conference. CD-ROM.
- Ferrari A. C. and Robertson J. 2000. Interpretation of Raman spectra of disordered and amorphous carbon. *Physical Review B—Condensed Matter and Materials Physics* 61:14095–14107.
- Frick U. and Pepin R. O. 1981. On the distribution of noble gases in Allende: A differential oxidation study. *Earth and Planetary Science Letters* 56:45–63.
- Huss G. R. 1990. Ubiquitous interstellar diamond and SiC in primitive chondrites: Abundances reflect metamorphism. *Nature* 347:159–162.
- Huss G. R. and Lewis R. S. 1994. Noble gases in presolar diamonds I: Three distinct components and their implications for diamond origins. *Meteoritics* 29:791–810.
- Huss G. R., Lewis R. S., and Hemkin S. 1996. The “normal planetary” noble gas component in primitive chondrites: Compositions, carrier, and metamorphic history. *Geochimica et Cosmochimica Acta* 60:3311–3340.
- Kagi H., Tsuchida I., Wakatsuki M., Takahashi K., Kamimura N., Iuchi K., and Wada H. 1994. Proper understanding of down-shifted Raman spectra of natural graphite: Direct estimation of laser-induced rise in sample temperature. *Geochimica et Cosmochimica Acta* 58:3527–3530.
- Lewis R. S., Srinivasan B., and Anders E. 1975. Host phase of a strange xenon component in Allende. *Science* 190:1251–1262.
- Marrocchi Y., Derenne S., Marty B., and Robert F. 2005. Interlayer trapping of noble gases in insoluble organic matter of primitive meteorites. *Earth and Planetary Science Letters* 236:569–578.
- Matsuda J., Lewis R. S., Takahashi H., and Anders E. 1980. Isotopic anomalies of noble gases in meteorites and their origins—VII. C3V carbonaceous chondrites. *Geochimica et Cosmochimica Acta* 44:1861–1874.
- Matsuda J., Amari S., and Nagao K. 1999. Purely physical separation of a small fraction of the Allende meteorite that is highly enriched in noble gases. *Meteoritics & Planetary Science* 34:129–136.
- Matsuda J., Namba M., Maruoka T., Matsumoto T., and Kurat G. 2005. Primordial noble gases in a graphite-metal inclusion from the Canyon Diablo IAB iron meteorite and their implications. *Meteoritics & Planetary Science* 40:431–443.
- Matsuda J., Morishita K., Nara M., and Amari S. 2009. Raman spectroscopic study of the noble gas carrier Q in the Allende meteorite. *Geochemical Journal* 43:323–329.
- Matsuda J., Amari S., Morishita K., Nagashima K., and Nara M. 2010a. The effect of pyridine treatment on phase Q: Orgueil and Allende. *Meteoritics & Planetary Science* 45:1191–1205.
- Matsuda J., Tsukamoto H., Miyakawa C., and Amari S. 2010b. Noble gas study of the Saratov L4 chondrite. *Meteoritics & Planetary Science* 45:361–372.
- Matsuda J., Morishita K., Tsukamoto H., Miyakawa C., Nara M., Amari S., Uchiyama T., and Takeda S. 2010c. An attempt to characterize phase Q: Noble gas, Raman spectroscopy and transmission electron microscopy in residues prepared from the Allende meteorite. *Geochimica et Cosmochimica Acta* 74:5398–5409.
- Moniot R. K. 1980. Noble-gas-rich separates from ordinary chondrites. *Geochimica et Cosmochimica Acta* 44: 253–271.
- Morishita K., Nara M., Amari S., and Matsuda J. 2011. On the effect of laser-induced heating in a Raman spectroscopic study of carbonaceous material in meteorite. *Spectroscopy Letters* 44:459–463.
- Nagashima K., Nara M., and Matsuda J. 2012. Raman spectroscopic study of diamond and graphite in ureilites and the origin of diamonds. *Meteoritics & Planetary Science* 47:1728–1737.
- Ott U., Mack R., and Chang S. 1981. Noble-gas-rich separates from the Allende meteorite. *Geochimica et Cosmochimica Acta* 45:1751–1788.
- Ozima M. and Podosek F. A. 1983. *Noble gas geochemistry*. Cambridge: Cambridge University Press. 367 p.
- Reynolds J. H., Frick U., Neil J. M., and Phinney D. L. 1978. Rare-gas-rich separates from carbonaceous chondrites. *Geochimica et Cosmochimica Acta* 42:1775–1797.
- Schelhaas N., Ott U., and Begemann F. 1990. Trapped noble gases in unequilibrated ordinary chondrites. *Geochimica et Cosmochimica Acta* 54:2869–2882.
- Schultz L., Weber H. W., and Begemann F. 1991. Noble gases in H-chondrites and potential differences between Antarctic and non-Antarctic meteorites. *Geochimica et Cosmochimica Acta* 55:59–66.
- Spring N., Vogel N., Baur H., Wieler R., Alexander C. M. O’D., and Busemann H. 2010. Pyridine treatment of insoluble organic matter from chondrites Krymka and Vigarano—No effects on the noble gas carrier phase Q (abstract #2640). 41st Lunar and Planetary Science Conference. CD-ROM.
- Spring N., Busemann H., Vogel N., Huber L., Wieler R., Maden C., and Alexander C. M. O’D. 2011. The susceptibility of phase Q to pyridine: Are CI chondrites unique? (abstract #5527). *Meteoritics & Planetary Science* 46:A220.
- Tuinstra F. and Koenig J. L. 1970. Raman spectrum of graphite. *The Journal of Chemical Physics* 53:1126–1130.
- Verchovsky A. B., Sephton M. A., Wright I. P., and Pillinger C. T. 2002. Separation of planetary noble gas carrier from bulk carbon in enstatite chondrites during stepped combustion. *Earth and Planetary Science Letters* 199:243–255.
- Wieler R., Anders E., Baur H., Lewis R. S., and Signer P. 1991. Noble gases in “phase Q”: Closed-system etching of an Allende residue. *Geochimica et Cosmochimica Acta* 55:1709–1722.
- Wieler R., Anders E., Baur H., Lewis R. S., and Signer P. 1992. Characterisation of Q-gases and other noble gas components in the Murchison meteorite. *Geochimica et Cosmochimica Acta* 56:2907–2921.